Structural Engineering and Mechanics, *Vol. 54, No. 4 (2015) 741-754*
DOI: http://dx.doi.org/10.12989/sem.2015.54.4.741

Prediction of engineering demand parameters for RC wall structures

Florin Pavel*[1] and Andrei Pricopie[2a]

[1]*Department of Reinforced Concrete Structures, Technical University of Civil Engineering Bucharest, Bd. Lacul Tei no. 122-124, Sector 2, 020396, Bucharest, Romania*
[2]*Department of Strength of Materials, Technical University of Civil Engineering Bucharest, Bd. Lacul Tei no. 122-124, Sector 2, 020396, Bucharest, Romania*

(Received May 5, 2014, Revised February 23, 2015, Accepted April 4, 2015)

Abstract. This study evaluates prediction models for three EDPs (engineering demand parameters) using data from three symmetrical structures with RC walls designed according to the currently enforced Romanian seismic design code P100-1/2013. The three analyzed EDPs are: the maximum interstorey drift, the maximum top displacement and the maximum shear force at the base of the RC walls. The strong ground motions used in this study consist of three pairs of recordings from the Vrancea intermediate-depth earthquakes of 1977, 1986 and 1990, as well as two other pairs of recordings from significant earthquakes in Turkey and Greece (Erzincan and Aigion). The five pairs of recordings are rotated in a clockwise direction and the values of the EDPs are recorded. Finally, the relation between various IMs (intensity measures) of the strong ground motion records and the EDPs is studied and two prediction models for EDPs are also evaluated using the analysis of residuals.

Keywords: strong ground motion records; interstorey drift; top displacement; shear force; prediction model

1. Introduction

This paper focuses on the assessment of the relation between three EDPs (engineering demand parameters) and several IMs (intensity measures) of strong ground motions for three RC walls structures designed according to the current Romanian seismic design code P100-1/2013. Five pairs of horizontal recordings (three from Romania, one from Greece and one from Turkey) are rotated in a clockwise direction every 5^{o} from 0^{o} to 180^{o}. Each pair of rotated strong ground motion recordings is used in the nonlinear time history analyses (NTHA) of the three RC walls structures. For each NTHA, three EDPs are recorded: maximum interstorey drift, maximum top displacement and maximums shear force at the base of the RC walls. The relations between the EDPs and the IMs is studied in the final part of this study.

The influence of rotating strong ground motion records on several EDPs has been recently

*Corresponding author, Assistant Professor, E-mail: florin.pavel@utcb.ro
[a]Assistant Professor, E-mail: andrei_pricopie@yahoo.com

http://www.techno-press.org/?journal=sem&subpage=8 ISSN: 1225-4568 (Print), 1598-6217 (Online)

studied by Reyes and Kalkan (2013), Kalkan and Reyes (2013), Kalkan and Kwong (2014) for both SDOFs (single-degree-of-freedom-systems) and MDOFs (multi-degree-of-freedom-systems). These studies show that there is no optimal angle which maximizes the values of all EDPs at the same time. Athanatopoulou (2005) proposed an analytical formulae for computing the critical incidence angle of the horizontal recordings so as to maximize or minimize the values of any response parameter. Rigato and Medina (2007) investigated the effect of the angle of incidence on several EDPs for a single storey structure (either torsionally balanced or torsionally unbalanced). This study shows that the peak inelastic displacement demands are underestimated when the horizontal components of the ground motion are applied only along the principal axes of the structures. In addition, the damage assessment of an inelastic structure is dependent on the angle of incidence of the ground motion.

In the report PEER 2009/01 (Watson-Lamprey 2009), a predictive equation for evaluating the median interstorery drift response is proposed. The relation is derived from NTHA performed on four structures (three RC frame structures and one RC wall structure). An equivalent linearization procedure is developed in the study of Günay and Sucuoğlu (2009) in order to predict the inelastic seismic response (e.g., roof displacements, interstorey drifts, chord rotations, shear forces) of a capacity designed RC frame structure. An evaluation of the current prescriptions in seismic design codes used for calculating the peak shear strength of low-aspect ratio RC walls is shown in the work of Del Carpio Ramos *et al.* (2012). Baker and Cornell (2008) developed vector-valued intensity measures for the prediction of structural response. Two IMs were analyzed in the study of Baker and Cornell (2008), namely the spectral acceleration corresponding to the fundamental eigenmode and a measure of the spectral shape which is the ratio between the spectral acceleration corresponding to the second eigenmode and the spectral acceleration corresponding to the fundamental eigenmode. Romão *et al. (*2012a, b) evaluate the performance (central value and dispersion) of 50 estimators of structural demand under earthquake loading. The relation between the collapse ratio of particular types of structures and four IMs (PGA – peak ground acceleration, PGV - peak ground velocity, PSA- peak spectral acceleration and PPSV- peak pseudo spectral velocity) is investigated in Wang *et al.* (2011) using data from the 2008 Wenchuan earthquake. Zhai *et al.* (2013) discuss the selection of the most unfavorable strong ground motion record for low-rise and medium-rise RC frame structures by assessing the performance of several IMs. Nguyen and Kim (2013), Canagallo *et al.* (2015) evaluate the influence of the incidence angles of earthquake ground motions on the response of either asymmetric single strorey structures or 3D reinforced concrete structures. Hancock and Bommer (2007) show that the duration of the strong ground motion is not correlated with different parameters related to the peak response and that it is correlated with the parameters related to cumulative damage, such as hysteretic energy or fatigue damage. Finally, a study of the relation between 23 IMs and 4 response parameters for 90 earthquake recordings is given in the study of Riddell (2007).

2. Strong ground motion dataset

In this study five pairs of horizontal strong ground motion recordings are used in order to evaluate the relation between several IMs and three EDPs for three RC walls structures designed according to the current Romanian seismic design code P100-1/2013.

The first three pairs of recordings: INCERC, Petresti and Campina were obtained during three Vrancea intermediate-depth seismic events in 1977, 1986 and 1990. According to the study of

Table 1 Characteristics of strong ground motions from Romania

Pairno.	Earthquake name	Station	Year	M_W	R (km)	Soil class (EC8)	Comp. 1		Comp. 2	
							PGA (cm/s^2)	PGV (cm/s)	PGA (cm/s^2)	PGV (cm/s)
1	Vrancea	INCERC	1977	7.4	101	C	206.9	70.5	188.5	30.8
2	Vrancea	Petresti	1986	7.1	64	C	273.3	36.5	297.1	32.0
3	Vrancea	Campina	1990	6.9	120	B	270.6	27.4	226.6	19.1

Table 2 Characteristics of strong ground motions from Greece and Turkey

Pairno.	Earthquake name	Station	Year	M_W	R (km)	Soil class (EC8)	Comp. 1		Comp. 2	
							PGA (cm/s^2)	PGV (cm/s)	PGA (cm/s^2)	PGV (cm/s)
4	Erzincan	Erzincan	1992	6.7	9	C	381.5	101.8	502.9	71.8
5	Aigion	Aigion OTE	1995	6.4	7	B	489.7	39.3	512.8	51.6

Pavel *et al.* (2013), these three strong ground motions (denoted as INC, PET and CMN) are the only recordings from Romania which exhibit near-field effects. The characteristics of these three strong ground motions are given in Table 1.

In addition to the three pairs of recordings from Romania, two other pairs of strong ground motion recordings from Greece (Aigion) and Turkey (Erzincan) are also used in this study. Table 2 shows some characteristics of the strong ground motion records from Aigion and Erzincan. The reason for using these two pairs of recordings is that they represent more extreme cases of seismic loading for structures. The peak ground acceleration values for these two recordings is superior to the values corresponding to the three pairs of Romanian recordings and is also superior to the design peak ground acceleration (considered as 0.25 g for the three analyzed buildings).

The I_{JMA} (Japan Meteorological Agency seismic intensity) is a seismic intensity scale based on all three recorded components of the strong ground motion (Shabestari and Yamazaki, 2001). The corresponding values of I_{JMA} for the five pairs of recordings are as follows: 5.9 for Erzincan recording, 5.8 for Aigion recording, 5.6 for INCERC recording, 5.4 for Petresti recording and 5.2 for Campina recording. The corresponding soil conditions for all the five pairs of recordings are defined according to the criteria from Eurocode 8 (2004), based on the average value of the shear wave velocity in the upper 30 m of soil deposits - $v_{s,30}$.

The five pairs of recordings are rotated each 5º from 0º to 180º. The mean absolute acceleration response spectra obtained from all the rotated components is compared in Fig. 1 with the elastic design spectrum from the Romanian seismic design code P100-1/2013 and which was used for the design of the three RC walls structures (PGA=0.25 g and control period T_C=1.0 s). The design spectrum in the Romanian seismic design code P100-1/2013 is characterized by three control periods: T_B=0.2·T_C=0.2 s, T_C=1.0 s and T_D=3.0 s and by a maximum dynamic amplification factor of 2.5 (similar with the value in Eurocode 8 for rock conditions). The results from Fig. 1 show that the mean response spectra for the three pairs of recordings from Romania generally fall below the elastic design spectrum with the exception of some limited period range. On the contrary, the mean response spectra obtained from the two pairs of recordings from Greece and Turkey are above the elastic design spectrum for much broader period ranges. In the case of the Erzincan pair of recordings, the mean rotated response spectrum is above the code spectrum for the entire period range between 0-4 s.

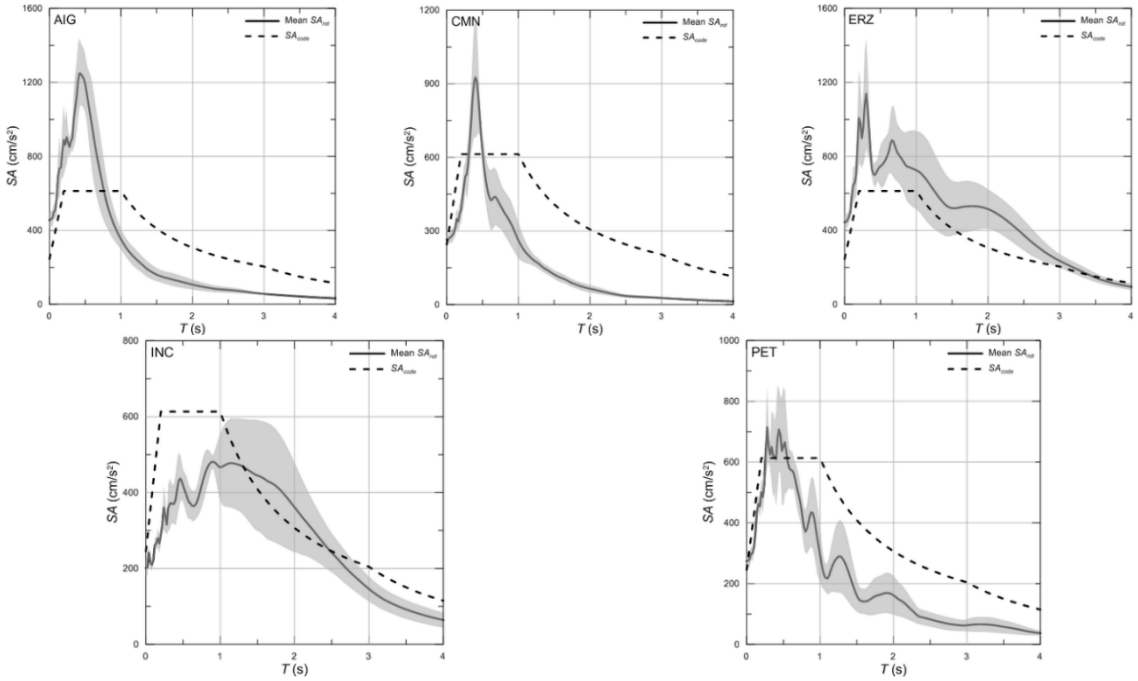

Fig. 1 Comparison of the mean absolute acceleration response spectra for all the rotated components with the absolute acceleration code elastic design spectrum (the shaded area corresponds to the mean plus one and minus one standard deviations absolute acceleration response spectra)

Table 3 Mean values of the selected IMs

Pair no.	Station	PGA (cm/s^2)	PGV (cm/s)	I_A (m/s)	CAV (cm/s)	ASI (cm/s)	VSI (cm)	T_M(s)
1	INCERC	201.1	48.2	0.68	591.2	138.9	181.7	1.16
2	Petresti	275.4	31.7	0.75	612.0	231.2	115.9	0.58
3	Campina	265.2	23.8	0.54	479.7	240.9	93.0	0.53
4	Erzincan	444.8	85.2	1.71	846.9	334.7	268.8	1.05
5	Aigion	455.9	41.6	1.09	527.7	387.8	150.7	0.50

Table 4 Coefficients of variation for the selected IMs

Pair no.	Station	COV						
		PGA	PGV	I_A	CAV	ASI	VSI	T_M
1	INCERC	0.10	0.34	0.19	0.06	0.07	0.20	0.16
2	Petresti	0.09	0.11	0.10	0.06	0.08	0.17	0.13
3	Campina	0.08	0.16	0.11	0.05	0.10	0.10	0.10
4	Erzincan	0.09	0.23	0.21	0.08	0.14	0.16	0.19
5	Aigion	0.09	0.15	0.06	0.02	0.08	0.06	0.03

The mean values and the coefficients of variation (COV) for several IMs for the rotated pairs of recordings are reported in Tables 3 and 4. The selected IMs are: peak ground acceleration (PGA), peak ground velocity (PGV), Arias Intensity - I_A (Arias 1970), cumulative absolute velocity- CAV

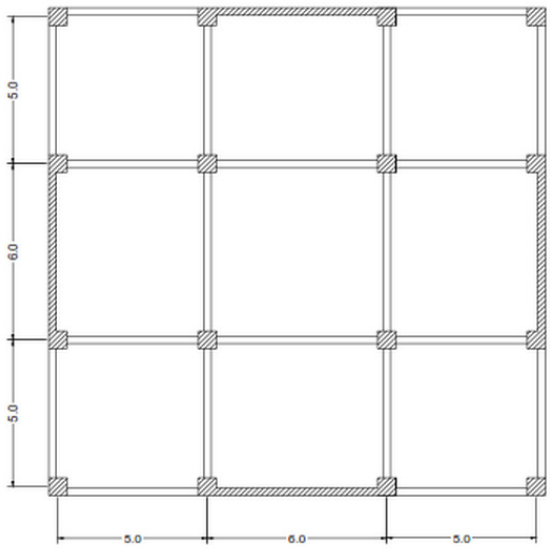

Fig. 2 Plan layout for the three analyzed RC wall structures

(EPRI 1988), acceleration spectrum intensity- ASI (Von Thun *et al.* 1988), velocity spectrum intensity- VSI (Von Thun *et al.* 1988) and mean period - T_M (Rathje *et al.* 1998).

One can notice from Table 3 that there are large differences between the mean values of the IMs for the five pairs of horizontal recordings. In addition, the large coefficients of variation encountered for PGV, VSI or T_M are also noticeable as is the constant variability encountered for PGA, CAV or ASI.

3. Structural models

Three doubly symmetrical RC walls structures are analyzed in this study. The first structure has six storeys (denoted hereinafter S6), the second structure has eight storeys (S8) and the last structure has ten storeys (S10). The structures are 17×17 m (2×5.0 m+1×6.0 m) in plane. The storey height is constant throughout the entire height of the building and is equal to 3 m. The layout in plane is similar for all the structures and is shown in Fig. 1.

The structural design is performed according to the prescriptions given in the current Romanian seismic design code P100-1/2013. Some additional design requirements are also given in the Romanian code for the design of RC structural wall buildings CR 2-1-1.1/2013.

The elastic spectrum used for design purposes is characterized by a peak ground acceleration of 0.25 g and a control period T_C=1.0 s. The design is performed for ductility class high (DCH) using a behavior factor q equal to 4. The total load at the level of the slab is taken as 13 kN/m^2 (including the effect of vertical loading). The slab is considered as rigid in its plane with a thickness of 15 cm. The structural system for all three buildings consists of four RC walls of 6 m in length (two in each direction), as well as columns and beams. The thickness of the web of the walls is the same for all three structures and is equal to 25 cm. The cross-section of all the structural elements is similar for all three buildings and is constant throughout the building height. The boundary

Table 5 Description of the structural elements

Struct.	Structural element					
	Structural walls		Columns		Beams	
	Cross-section/thickness	Long. reinf. ratio (%)	Cross-section	Long. reinf. ratio (%)	Cross-section	Long. reinf. ratio (%)
S6	boundary – 60×60 cm web – 25 cm	boundary – 0.80 % - 1.24 % web – 0.31 %	60×60 cm	1.05 %	25×60 cm	0.40 % – 0.63 %
S8	boundary – 60×60 cm web – 25 cm	boundary – 0.80 % - 1.78 % web – 0.31 % - 0.45 %	60×60 cm	1.05 %	25×60 cm	0.40 % – 0.78 %
S10	boundary – 60×60 cm web – 25 cm	boundary – 0.80 % - 2.46 % web – 0.31 % - 0.53 %	60×60 cm	1.05 %	25×60 cm	0.63 % – 0.98 %

elements at the edges of the RC walls have the same cross-sectional dimensions as the columns. The materials used are concrete class C30/37 and steel grade S500C. A brief description of the structural elements (including reinforcement ratios) can be found in Table 5. The transversal reinforcement used for all the structural elements (structural walls, columns and beams) is computed based on capacity-design principles as recommended by the Romanian code for the design of RC structural wall buildings CR 2-1-1.1/2013. As such, both the diagonal compression and diagonal tension failure mechanisms are precluded. The transversal reinforcement in the structural walls varies from 2×Ø12/12.5 cm (or 2×Ø10/12.5 cm for the S6 structure) at the bottom part up to 2×Ø8/15 cm at the top part of the wall (minimum code specified transversal reinforcement). The transversal reinforcement in the boundary elements of the structural walls was designed taking into account the wall transversal reinforcement area, as well as the spacing and minimum area conditions imposed by the Romanian code for the design of RC structural wall buildings CR 2-1-1.1/2013. The sliding shear check is also passed by all the analyzed structural walls.

The fundamental eigenperiods using cracked RC sections are 0.37 s for S6 structure, 0.56 s for the S8 structure and 0.76 s for the S10 structure and 0.29 s, 0.41 s and 0.55, respectively when using uncracked RC sections.

The NTHA are performed using STERA3D software. The basic assumptions of the NTHA are described subsequently. All the structural elements are considered as line elements and the floor diaphragms are modelled as rigid in their plane. The beams are modelled as elements with nonlinear flexural hinges at both ends and a nonlinear shear hinge in the middle of the element. The column elements is modelled using a multi spring (MS) model with nonlinear axial springs at both ends and bi-directional nonlinear shear springs in the middle. The wall element is similar with the column element, consisting of both nonlinear axial springs and shear springs in both the boundary elements and in the wall web. In addition, the wall element has rigid beams at the top and at the bottom of the element. The additional effect of the slab is taken into account in the modelling of the beam elements. The hysteretic model of the beam elements is based on a trilinear model which can account for strength degradation, stiffness degradation and for slip degradation, as well. The multi spring (MS) model for the vertical elements consists of five areas – the four

Table 6 Correlation coefficients between EDPs and IMs

EDP	Correlation coefficients						
	PGA	PGV	I_A	CAV	ASI	VSI	T_M
Maximum interstorey drift $\theta_{\max}$	0.59	0.69	0.76	0.57	0.50	0.63	0.20
Maximum top displacement $d_{\max}$	0.47	0.60	0.64	0.50	0.38	0.55	0.21
Maximum wall base shear force $V_{b,\max}$	0.62	0.76	0.80	0.67	0.48	0.73	0.32

corner areas have both concrete and steel nonlinear springs, while the central area has only a nonlinear concrete spring. The concrete and steel strengths are based on mean strengths of the materials taking into account also the concrete confinement and the steel consolidation. The tension strength of the concrete is neglected in the analyses. In the case of the steel nonlinear springs, the maximum-oriented model is adopted prior to yielding and a trilinear model is adopted afterwards. The trilinear hysteresis rule is also adopted for the concrete springs with consideration of the strength degradation after the yielding point. A Rayleigh damping model is used in the computations, with a damping of 5% for the first eigenmode. It is obvious that there are more complex models available in literature able to account for many other features characteristic to the seismic behavior of RC walls structures, but it is beyond the scope of this paper to compare and select the most appropriate modelling approach or to test it. For guidance, some other modelling techniques for RC structural walls can be found in Kappos and Antoniadis (2011), Kazaz *et al.* (2012), Belletti *et al.* (2013) or Valoroso *et al*. (2014).

4. Results

The results of the NTHA performed in STERA software and using the main assumptions shown in the previous chapter are presented and discussed in the ensuing sections. As previously mentioned, three EDPs are investigated: the maximum interstorey drift (denoted as $\theta_{\max}$), the maximum displacement at the top of the structure (denoted as $d_{\max}$) and the maximum shear force at the base of the RC walls (denoted as $V_{b,\max}$).

Table 6 shows the values of the coefficients of correlation between the three EDPs and the IMs shown in Chapter 2 (see Table 3 and 4). It is noteworthy from Table 6 the fact that the best coefficients of correlation are obtained for the maximum wall base shear force and the smallest ones for the maximum top displacement. In addition, two IMs, namely PGV and I_A provide the best correlations with the three analyzed EDPs.

Watson-Lamprey (2009) proposed a predictive equation for the median inter-storey drift, having the functional form given below

$$\ln EDP = b_1 + b_2 InSa_{T1} + b_3 InSa_{T1}^2 + b_4 InSa_{2T1} + b_5 InSa_{2T1}^2 + b_6 InSa_{T2} + b_7 InSa_{T2}^2 \quad (1)$$

The relation given above appears very appealing from the engineering point of view because it requires only parameters which can be derived from a probabilistic seismic hazard assessment of a particular site of interest. In this study two functional forms will be tested: the first functional form is the one given in relation (1) for which the parameters b_1–b_7 will be recalibrated using the data

Table 7 Regression models coefficients

Coefficient	Rel. (1)			Rel. (2)		
	$V_{b,\max}$	$d_{\max}$	$\theta_{\max}$	$V_{b,\max}$	$d_{\max}$	$\theta_{\max}$
b_1	-6332.00	-41.59	-2.12	-5638.73	-34.26	-1.88
b_2	109.48	-0.81	-0.47	204.41	0.20	-0.44
b_3	55.24	0.10	0.27	102.70	0.60	0.28
b_4	277.00	0.18	-0.45	122.67	-1.45	-0.51
b_5	139.00	0.59	0.27	61.84	-0.23	0.25
b_6	393.95	3.21	-0.37	222.71	1.40	-0.43
b_7	197.48	2.11	0.31	111.85	1.20	0.28
b_8	-	-	-	533.52	5.64	0.19

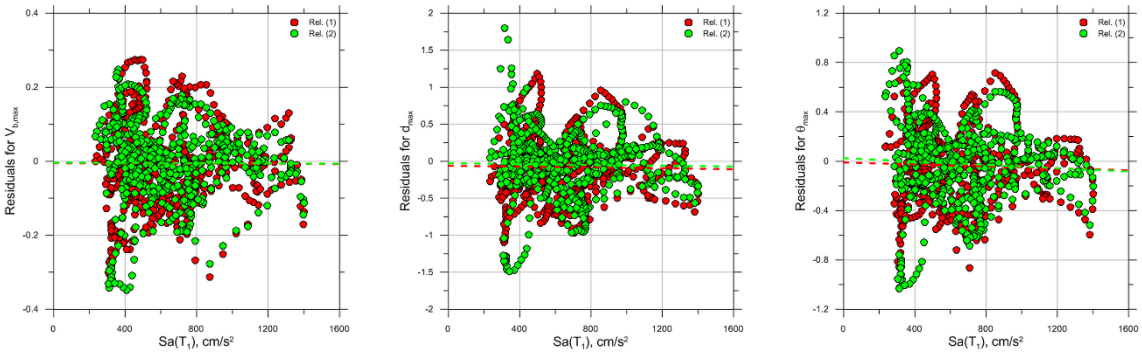

Fig. 3 Distribution of residuals obtained applying Rel. (1) and (2) for the three analyzed EDPs as a function of Sa(T1)

from NTHA for all three EDPs and a second functional form in which another term related to PGV is introduced. The second functional form is given in relation (2) below

$$\ln EDP = b_1 + b_2 InSa_{T1} + b_3 InSa_{T1}^2 + b_4 InSa_{2T1} + b_5 InSa_{2T1}^2 + b_6 InSa_{T2} + b_7 InSa_{T2}^2 + b_8 \ln PGV \quad (2)$$

In Rel. (1) and (2), Sa_{T1} and Sa_{T2} represent the spectral acceleration corresponding to the first and second eigenperiod of the structures and Sa_{2T1} is the spectral acceleration corresponding to a period which is equal to two times the first eigenperiod of the structure.

There are a number of relevant studies in literature (e.g., Campbell and Bozorgnia 2011, Bradley *et al.* 2009, Kempton and Stewart 2006, etc.) dealing with prediction models for other IMs, some of which are mentioned in Chapter 2 (e.g., CAV, SI, significant duration, etc.). However, one has to consider that these types of ground motion prediction models haven't been developed yet for Romania, whose seismicity is dominated by the Vrancea subcrustal seismic source. As such, only spectral accelerations and peak ground velocities can be obtained from seismic hazard studies for Romania. Therefore, only the two above-mentioned functional forms will be tested and compared in the next sections of this Chapter.

The first step in order to derive the parameters of the functional model is to select whether the model will use the EDPs computed using the cracked RC sections assumption or the ones for the uncracked RC sections. The correlations performed have shown that in this case, the larger values are obtained for the cracked RC sections. The differences between the values of the correlation

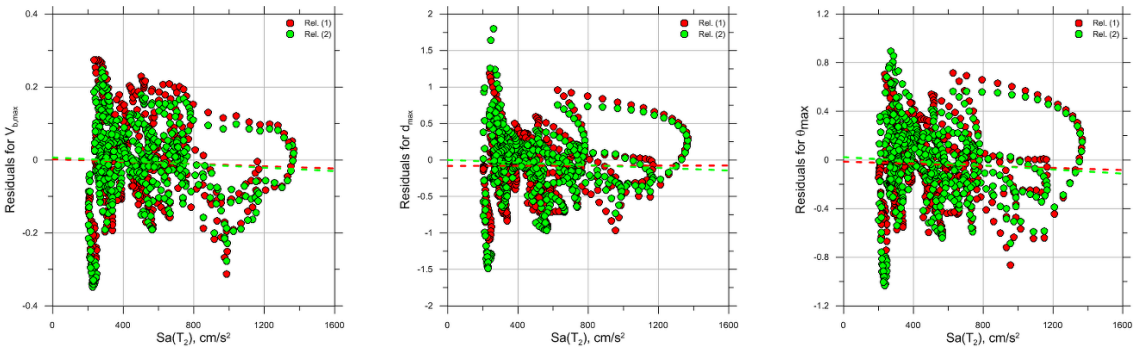

Fig. 4 Distribution of residuals obtained applying Rel. (1) and (2) for the three analyzed EDPs as a function of Sa(T2)

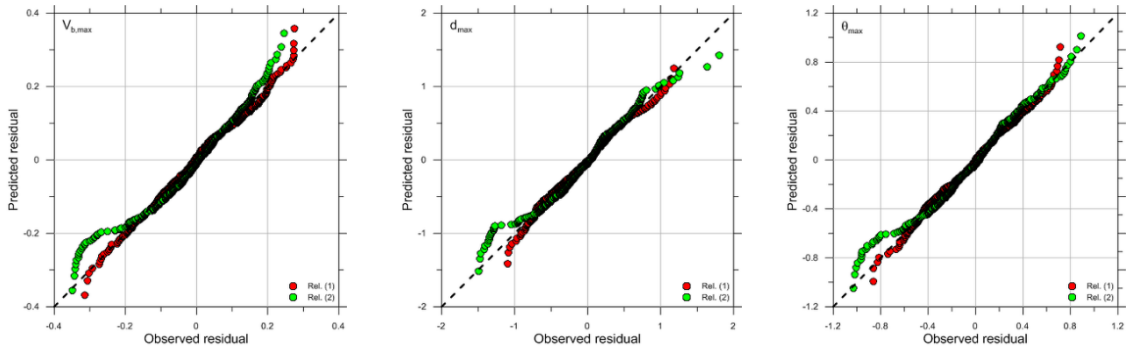

Fig. 5 Q-Q plots of the residuals for the three EDPs

coefficients for the two assumptions can be as high as 40% in some cases. The regression coefficients from b_1–b_7 and b_1–b_8, respectively are given in Table 7 for all three EDPs.

The regression coefficients for the inter-storey drift appear different than in the study of Watson-Lamprey (2009). However, one might consider the fact that in this case the larger coefficients of correlation between the EDPs and the selected IMs were obtained for the spectral acceleration corresponding to the second mode of vibration of the building, denoted as $Sa(T_2)$. This particular aspect will require further investigations in the future. In addition, one has to keep in mind that these results were obtained for symmetrical RC walls structures designed according to the Romanian seismic design code with periods ranging from 0.37–0.76 s and should not be extrapolated to other structures.

The residuals which represent the difference between the observed and predicted values for the two models given in Rel. (1) and (2) are plotted in Figs. 3-4 as a function of $Sa(T_1)$ and $Sa(T_2)$, which represent the spectral acceleration corresponding to the first and second eigenperiod of the structures. A trendline obtained from the values of the residuals is also fitted in Figs. 3 and 4 and is represented with the corresponding color.

One can notice from Figs. 3 and 4 that the smallest residuals are encountered for the maximum shear force at the base of the wall (residuals in the range –0.3 to +0.3), while the largest ones are encountered for the maximum top displacement (residuals in the range –2.0 to +2.0). No visible trend can be observed in the case of the distribution of the residuals with respect to $Sa(T_1)$, while there is a small, but noticeable trend of over-estimation in the case of the distribution with respect

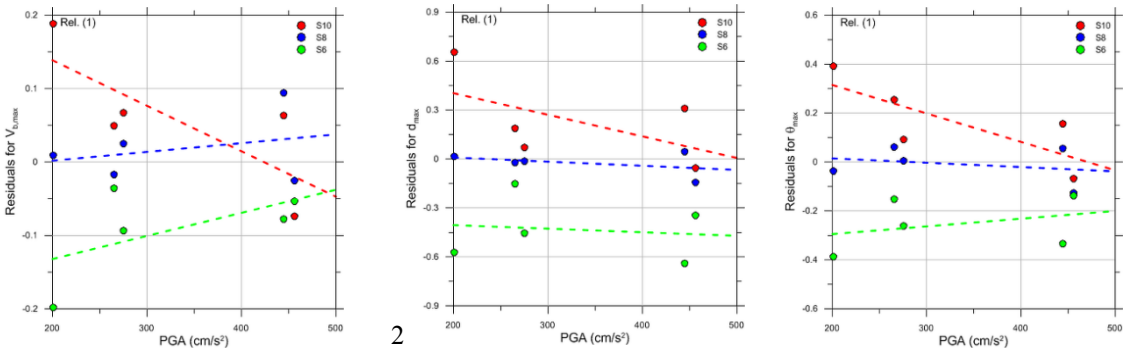

Fig. 6 Distribution of within-earthquake residuals for each structure obtained by applying Rel. (1) for the three analyzed EDPs as a function of PGA

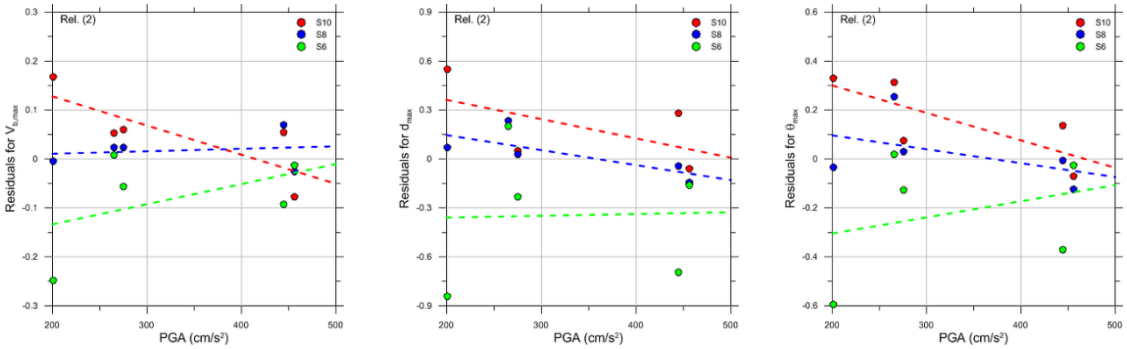

Fig. 7 Distribution of within-earthquake residuals for each structure obtained by applying Rel. (2) for the three analyzed EDPs as a function of PGA

to $Sa(T_2)$ for all three analyzed EDPs.

Fig. 5 displays the Q-Q plots computed using the normal probability distribution distribution of the residuals for the three EDPs for both relation (1) and relation (2). The Q-Q plots show whether the assumed normal probability distribution can be considered as adequate for the modelling of the distribution of the considered EDPs.

It is noticeable from Fig. 5 and Figs. 3 and 4, as well that relation (1) provides smaller values of the residuals. In order to better check the variability of the proposed relation, a within-earthquake residual was computed for each of the three analyzed structures and is plotted in Figs. 6 and 7 as a function of the mean rotated peak ground acceleration for each pair of recordings. The within-earthquake residual is similar to the intra-event residuals computed in the case of ground motion prediction models (e.g., Stafford *et al.* 2008) and used for the assessment of GMPEs (ground motion prediction equations). The intra-event residual represents an average value of the residual for each of the five analyzed earthquakes. The trendlines associated to the within-earthquakes residuals of each structure are also shown in Figs. 6 and 7, with the same color as the individual values.

The plots in Figs. 6 and 7 reveal a very interesting trend for all three EDPs. Both relation (1) and relation (2) provide under-estimations for all three EDPs in the case of structure S10 and over-estimations for structure S6. Structure S8 on the other hand exhibits residuals almost equal to 0 for the entire PGA range of interest. Moreover, one might notice the fact that the trendlines of both S6

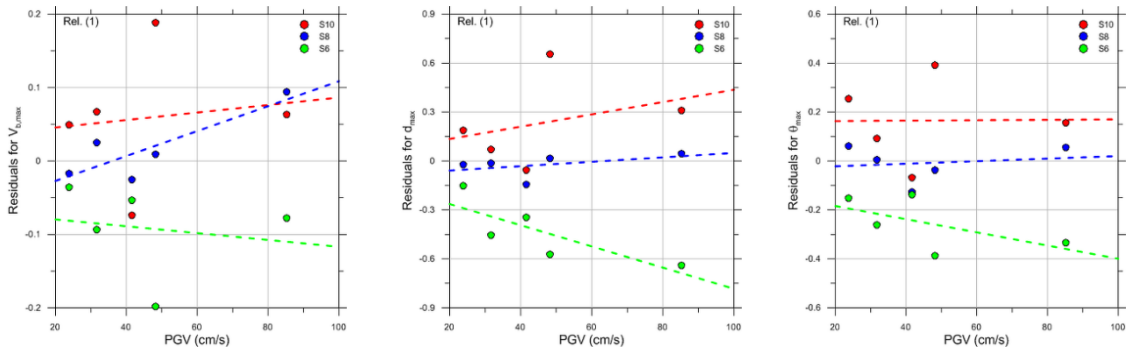

Fig. 8 Distribution of within-earthquake residuals for each structure obtained by applying Rel. (1) for the three analyzed EDPs as a function of PGV

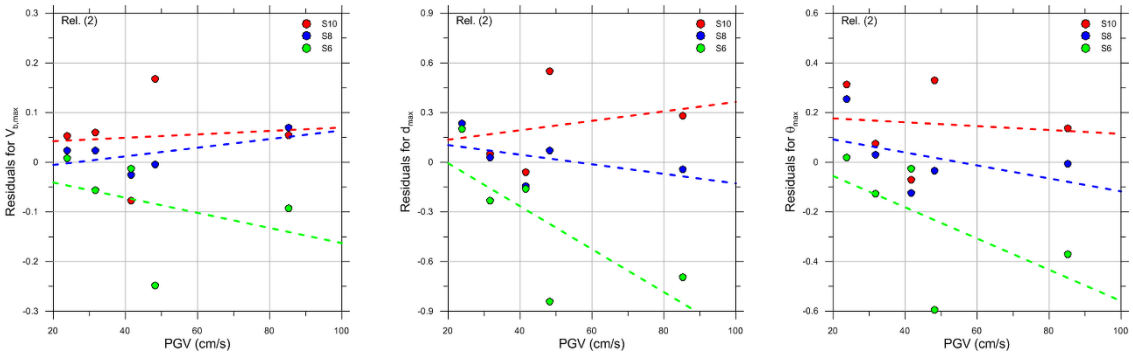

Fig. 9 Distribution of within-earthquake residuals for each structure obtained by applying Rel. (2) for the three analyzed EDPs as a function of PGV

and S10 structures are directed in almost all cases towards 0 (albeit the fact that the slope of the trendline is positive for S6 and negative for S10), showing that the level of under/over-estimation appears to decrease with the increasing PGA values.

The within-earthquake residuals' distribution is shown in Figs. 8 and 9 with respect to the peak ground velocity PGV. The previous observation related to the fact that the within-earthquake residuals are around 0 for structures S8 is confirmed by Figs. 8 and 9, as well. However, one can see that contrary to Figs. 6 and 7, in this case the predicted values for S6 and S10 move further away form 0 as PGV increases. There is also a change in the slopes of the fitted trendlines for strucutres S6 and S10 contrary to the results shown in Figs. 6 and 7. The smallest within-earthquake residuals are encountered for small PGV values and there is a trend of increasing residuals (of over- or under-estimation) as PGV increases.

Finally, one can conclude that the maximum base shear force at the base of the structural wall has the smallest associated variability, while the maximum top displacement has the highest variability. In addition, based on the above results, it appears that Rel. (1) is more adequate that Rel. (2) and the introduction of a parameter related to PGV does not improve the overall prediction results. Nevertheless, one has to keep in mind the fact that these relations were derived from a rather limited number of earthquake recordings (only five pairs of horizontal recordings), albeit the overall number of rotated strong ground motion recordings is in excess of 500 and that the sample of structures is limited, too (only three symmetrical structures). As such, these relations are

structure-dependent and should not be used for other structures unless additional specific studies will be conducted.

5. Conclusions

The main focus of this study is to check the relation between various IMs (intensity measures) of rotated strong ground motions and three EDPs (engineering demand parameters) for three RC walls structures designed according to the currently enforced Romanian seismic design code. The three selected EDPs are: the maximum interstorey drift (denoted as θ_{max}), the maximum displacement at the top of the structure (denoted as d_{max}) and the maximum shear force at the base of the RC walls (denoted as $V_{b,max}$). The strong ground motion database consists of five pairs of horizontal recordings obtained during three earthquakes originating from the Vrancea subcrustal seismic source in Romania and from two earthquakes in Turkey and Greece which were rotated each 5º from 0º to 180º. NTHA (Nonlinear time-history analyses) were conducted for each pair of rotated strong ground motion recordings using the software STERA3D.

The results of the analyses show that two IMs: PGV (peak ground velocity) and I_A (Arias intensity) provide the best correlation with the selected EDPs. Subsequently, predictive coefficients for the model of Watson-Lamprey (2009) are obtained for each EDP. In addition, a second model in which a specific term accounting for the peak ground velocity PGV was inserted is also tested. The analysis of the residuals for the two predictive models shows that the introduction of the PGV term did not improve the overall predictive capability of the model. In fact the introduction of the PGV term has increased the overall model variability. Among the three selected EDPs, the analyses have shown that the smallest variability is associated with the shear force at the base of the structural wall, while the largest variability is observed in the case of the maximum top displacement. The within-earthquake residuals show that as PGA increases, the values of the residuals decrease, while in the case of PGV an opposite trend is revealed.

Acknowledgments

The constructive feedback of one anonymous reviewer is greatly appreciated as it has helped us to improve considerably the quality of the manuscript.

References

Arias, A. (1970), "A measure of earthquake intensity", Ed. Hansen, R.J., *Seismic Design for Nuclear Power Plants*, MIT Press, Cambridge, Massachusetts.

Athanatopoulou, A.M. (2005), "Critical orientation of three correlated seismic components", *Eng. Struct.*, **27**(2), 301-312.

Baker, J.W. and Cornell, C.A. (2008), "Vector-valued intensity measures incorporating spectral shape for prediction of structural response", *J. Earthq. Eng.*, **12**(4), 534-554.

Belletti, B., Damoni, C. and Gasperi, A. (2013), "Modeling approaches suitable for pushover analyses of RC structural wall buildings", *Eng. Struct.*, **57**, 327-338.

Bradley, B.A., Cubrinovski, M., MacRae, G.A. and Dhakal, R.P. (2009), "Ground-motion prediction equation for SI based on spectral acceleration equations", *Bull. Seismol. Soc. Am.*, **99**(1), 277-285.

Campbell, K.W. and Bozorgnia, Y. (2011), "Prediction equations for the standardized version of cumulative absolute velocity for use in the shutdown of US nuclear power plants", *Nucl. Eng. Des.*, **241**, 2558-2569.
Cantagallo, C., Camataa, G. and Spacone, B. (2015), "Influence of ground motion selection methods on seismic directionality effects", *Earthq. Struct.*, **8**(1), 185-204.
CR 2-1-1.1/2013, *Design code for RC structural wall building*, Ministry of Regional Development and Public Administration, Bucharest, Romania.
Del Carpio Ramos, M., Whittaker, A.S. and Gulec, C.K. (2012), "Predictive equations for the peak shear strength of low-aspect ratio reinforced concrete walls", *J. Earthq. Eng.*, **16**(2), 159-187.
EPRI - Electrical Power Research Institute (1988), "A criterion for determining exceedance of the operating basis earthquake", Report no. EPRI NP-5930, Palo Alto, California.
Eurocode 8 (2004), *Design of structures for earthquake resistance, Part I: general rules, seismic actions and rules for buildings*, CEN, Brussels, Belgium.
Günay, M.S. and Sucuoğlu, H. (2009), "Predicting the seismic response of capacity-designed structures by equivalent linearization", *J. Earthq. Eng.*, **13**(5), 623-649.
Hancock, J. and Bommer, J.J. (2007), "Using spectral matched records to explore the influence of strong-motion duration on inelastic structural response", *Soil Dyn. Earthq. Eng.*, **27**(4), 291-299.
Kalkan, E. and Reyes, J.C. (2013), "Significance of rotating ground motions on behavior of symmetric- and asymmetric-plan structures: part 2. Case studies", *Earthq. Spectra*, doi: 10.1193/072012EQS242M.
Kalkan, E. and Kwong, N.S. (2014), "Pros and cons of rotating ground motions records to fault normal/parallel directions for response history analysis of buildings", *J. Struct. Eng.*, **140**(3), 04013062.
Kappos, A.J. and Antoniadis, A. (2011), "Evaluation and suggestions for improvement of seismic design procedures for R/C walls in dual systems", *Earthq. Eng. Struct. Dyn.,* **40**(1), 35-53.
Kazaz, I., Gülkan, P. and Yakut, A. (2012), "Deformation limits for structural walls with confined boundaries", *Earthq. Spectra*, **28**(3), 1019-1046.
Kempton, J.J. and Stewart, J.P. (2006), "Prediction equations for significant duration of earthquake ground motions considering site and near-source effects", *Earthq. Spectra*, **22**(4), 985-1013.
Nguyen, V.T. and Kim, D. (2013), "Influence of incident angles of earthquakes on inelastic responses of asymmetric-plan structures", *Struct. Eng, Mech*., **45**(3), 373-389.
P100-1/2013, *Code for seismic design – Part I – Design prescriptions for buildings*, Ministry of Regional Development and Public Administration, Bucharest, Romania.
Pavel, F., Aldea, A. and Vacareanu, R. (2013), "Near-field strong ground motions records from Vrancea earthquakes", *Proceedings of the International Conference on Earthquake Engineering SE-50 EEE*, Skopje, Macedonia.
Rathje, E.M., Abrahamson, N.A. and Bray, J.D. (1998), "Simplified frequency content estimates of earthquake ground motions", *J. Geotech. Geoenviron. Eng.*, **124**(2), 150-159.
Reyes, J.C. and Kalkan, E. (2013), "Significance of rotating ground motions on behavior of symmetric- and asymmetric-plan structures: part 1. Single story structures", *Earthq. Spectra*, doi: 10.1193/072012EQS241M.
Riddell, R. (2007), "On ground motion intensity indices", *Earthq. Spectra*, **23**(1), 147-173.
Rigato, A.B. and Medina, R.A. (2007), "Influence of angle of incidence on seismic demands for inelastic single-storey structures subjected to bi-directional ground motions", *Eng. Struct.*, **29**(10), 2593-2601.
Romão, X., Delgado, R. and Costa A. (2012a), "Statistical characterization of structural demand under earthquake loading. Part 1: robust estimation of the central value of the data", *J. Earthq. Eng.*, **16**(6), 686-718.
Romão, X., Delgado, R. and Costa A. (2012a), "Statistical characterization of structural demand under earthquake loading. Part 1: robust estimation of the dispersion of the data", *J. Earthq. Eng.*, **16**(6), 864-896.
Shabestari, K. and Yamazaki, F. (2001), "A proposal of instrumental seismic intensity scale compatible with MMI evaluated from three-component acceleration records", *Earthq. Eng. Struct. Dyn.*, **17**(4), 711-723.
Stafford, P.J., Strasser, F.O. and Bommer, J.J. (2008), "An evaluation of the applicability of the NGA models to ground-motion prediction in the Euro-Mediterranean region", *Bull. Earthq. Eng.*, **6**(2), 149-177.

Valoroso, N., Marmo, F. and Sessa, S. (2014), "Limit state analysis of reinforced shear walls", *Eng. Struct.*, **61**, 127-139.

Von Thun, J.L., Roehm, L.H., Scott, G.A. and Wilson, J.A. (1988), "Earthquake ground motions for design and analysis of dams", Ed. Von Thun, J.L., *Earthquake Engineering and Soil Dynamics II - Recent Advances in Ground-Motion Evaluation*, Geotechnical Special Publication no. 20, 463-481.

Wang, X., Masaki, K. and Irikura, K. (2011), "Building damage criteria from strong ground motion characteristics during the 2008 Wenchuan earthquake", *J. Earthq. Eng.*, **15**(7), 1117-1137.

Watson-Lamprey, J. (2009), Chapter 4 "Point of comparison", Ed. Haselton, C., *Evaluation of ground motion selection and modification methods: predicting median interstorey drift response for buildings*, PEER Report 2009/01, Pacific Earthquake Engineering Center, College of Engineering, University of California, Berkeley.

Zhai, C., Chang, Z., Li, S. and Xie, L. (2013), "Selection of the most unfavorable real ground motions for low-and mid-rise RC frame structures", *J. Earthq. Eng.*, **17**(8), 1233-1251.

http://iisee.kenken.go.jp/net/saito/stera3d/

CC